THE BALTIC JOURNAL
OF ROAD AND BRIDGE ENGINEERING

ISSN 1822-427X / eISSN 1822-4288
2016 Volume 11(3): 188–196

ANALYSIS OF GUSSET PLATE OF CONTEMPORARY BRIDGE TRUSS GIRDER

Wojciech Siekierski

Institute of Civil Engineering, Poznań University of Technology, ul. Piotrowo 5, 61-138 Poznań, Poland
E-mail: wojciech.siekierski@put.poznan.pl

Abstract. Trussed structures in modern bridge building usually have "W" bracing. Structural joints are often based on application of gusset plates. Experimental tests of stress distribution in such gusset plates are rather sparse. Lab testing of scaled bridge truss girder was carried out in Poznań University of Technology in Poznań. Investigation into stress distribution in gusseted joint was carried out. Test results were put against results obtained from analyses of two finite element models: beam-element model and shell-element model. Normal stress and Huber-Mises equivalent stress distributions within gusseted joint were analysed. General conclusions are: a) normal stress distribution in gusseted joint cross-section, perpendicular to truss flange axis, is nonlinear and extreme stresses occur near cross-section edges, b) Huber-Mises equivalent stress distribution in the cross-section of gusset plate near its connection to truss flange is nonlinear and extreme stresses occur near centre of the cross-section, c) assessment of normal stresses in gusseted joints should not be carried out with an aid of beam-element modelling, d) it is possible to assess Huber-Mises equivalent stresses in gusset plate near its welded connection to rigid flange with an aid of beam-element modelling if non-uniform distribution of shear stress is taken into account, e) shell-element modelling of gusseted joint provides satisfactory accuracy of normal and equivalent stress assessment, f) beam-element modelling of friction grip bolts is sufficiently accurate for shell-element models of steel joints analysed within elastic range of behaviour.

Keywords: bridge truss girder, connection, finite element method (FEM), gusset plate, lab test, stress.

1. Joints of modern bridge truss girders

Modern bridge truss girders have usually "W" bracing and rigid flange at deck level, i.e. cross beams are connected to girder flange at nodes and between them (Ahlgrimm, Lohrer 2005). Described layout of girder makes erection and maintenance easier. Thanks to intermediate cross beams deck weight is reduced. The example of such span is shown in Fig. 1.

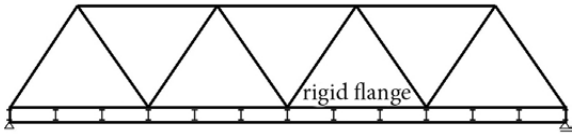

Fig. 1. Scheme of Warren truss with rigid bottom flange

Fig. 2. Truss-stayed bridge

The "W" bracing is applied also in truss-stayed bridges (Reintjes, Gebert 2006) and in trussed decks of modern cable-stayed bridges (Zongyu 2012) – Figs 2 and 3. The trussed decks often have rigid flanges.

Since rigid flanges must provide substantial flexural stiffness, they have cross-sections typical for beams, i.e. I or box. Bracing members are usually attached to flanges with an aid of twin gusset plates. Frequently each of gusset plate is butt welded to horizontal (top or bottom) plate of the truss flange. To reduce gusset plate dimensions flange theoretical axis is situated near the level of gusset plate – to – flange connection, instead of at the flange neutral axis. Thus, eccentricities occur. It is shown in Fig. 4 (bracing member axes projected on gusset plate plane are marked).

Fig. 3. Cable-stayed bridge with trussed deck

doi:10.3846/bjrbe.2016.22

Majority of available studies concern joints with single gusset plates in braced frames. Usually the joints situated at frame corner with single bracing member were analysed (Kaneko *et al.* 2008; Yoo *et al.* 2008). Frame connections of inverted V-braces (two bracings at joint) were also studied (Chou, Chen 2009; Zhang *et al.* 2011). In both cases gusseted joints were loaded due to frame sway. Beam bending was omitted. Studies completed for bridge joints concerned mainly rather obsolete joint layout with two bracing members and column meeting at a joint (Berman *et al.* 2010; Crosti, Duthinh 2012; Najjar, DeOrtentiis 2010). Experimental analyses of gusset plates in "W" braced bridge truss girder with rigid flange are hard to find.

The paper presents assorted results of testing of scaled truss girder with "W" bracing and some results of its finite element method (FEM) analyses.

2. Simplified stress analysis for gusset plates

2.1. Normal stress analysis

One of the oldest methods of gusset plate design is based on beam analogy. Part of truss flange together with gusset plate is analysed as a beam in bending and tension (or compression) at the same time (Szelągowski 1966) – Fig. 5.

Normal stress in the A-A cross-section of the gusset plate shown in Fig. 5 is calculated as follows:

$$\sigma = \frac{U_1 + D_1 \cos(\alpha)}{A} + \frac{\left[U_1 + D_1 \cos(\alpha)\right] e}{J} y, \qquad (1)$$

where U_1 – axial forces in truss flange, kN; D_1 – axial forces in bracing member, kN; e – distance between centre of gravity of the analysed cross-section and theoretical node of truss, m; y – distance between centre of gravity of the analysed cross-section and its respective edge fibre, m; α – angle between axes of truss flange and bracing member, (rad); A – cross-sectional area of analysed cross-section, m^2; J – moment of inertia of the analysed cross-section, m^4.

Beam analogy gives inaccurate assessment of stresses in gusset plates in terms of their magnitude and distribution.

More accurate method of gusset plate design is based on the Whitmore criterion (Whitmore 1952). It is applicable especially when gusset plate is connected to a member in tension. Extreme stress in gusset plate may be computed in a simplified way. The assumption is made that gusset plate carries stress over the width w. It is measured along the last row of rivets/bolts and it is set according to rules presented in Fig. 6. In the case of interference with other members connected to the gusset plate, the width w is limited by outer rivets/bolts that connect the other members. Applicability of this approach was confirmed by independent tests (Najjar, DeOrtentiis 2010; Rosenstrauch *et al.* 2013).

According to the Whitmore criterion, the representative normal stress in gusset plate is:

$$\sigma = \frac{N}{wt}, \qquad (2)$$

where N – axial force in truss member, kN; w – active width of gusset plate, m; t – thickness of gusset plate, m.

Gusset plate in tension may also be designed based on block shear idea. Current block shear criterion is based on the approach presented in (Hardash *et al.* 1985). Tearing line runs along outer rivets/bolts within the connection. It is shown in Fig. 7.

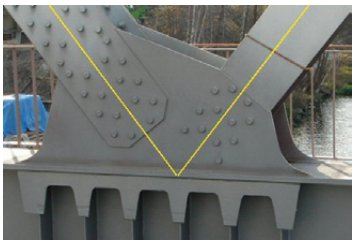

Fig. 4. Gusseted joint of bracing members and rigid flange

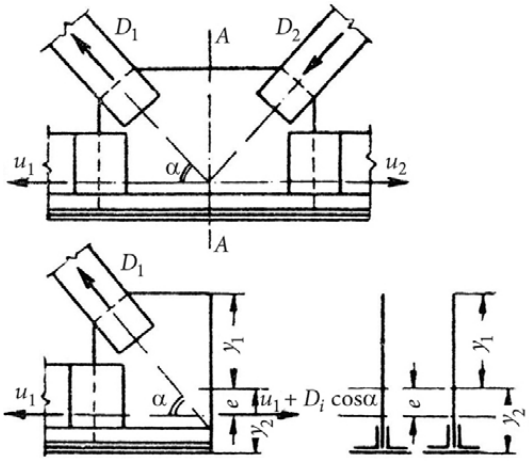

Fig. 5. Analysis of gusset plate based on beam analogy

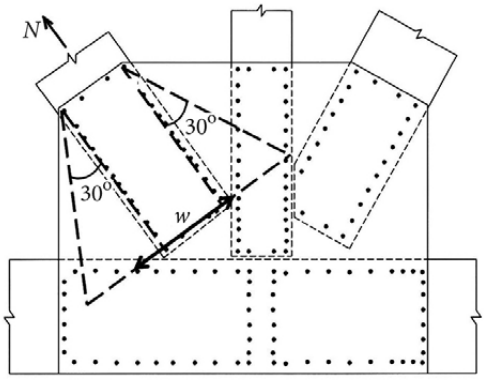

Fig. 6. Whitmore criterion of setting active gusset plate width

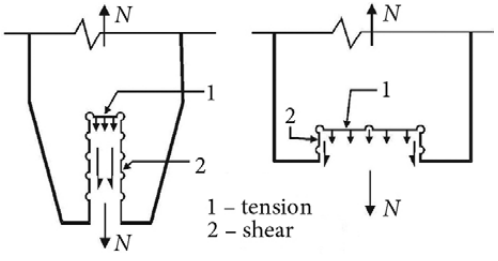

Fig. 7. Current concept of block shear in gusset plate

Current criterion of block shear specifies load carrying capacity as:

$$N_{\max} = A_t f_a + A_v f_{av}, \tag{3}$$

where A_t – net cross section of the part of gusset plate in tension, m^2; A_v – net cross section of the part of gusset plate in shear, m^2; f_a – steel yield strength in tension, MPa; f_{av} – steel yield strength in shear, MPa.

There are also simplified methods of design gusset plates connected to members carrying compression. If it is assured that buckling failure occurs before gusset plate yielding, a method based on column analogy may be applied (Thornton 1984). The method is shown in Fig. 8. Distance AB is the active width according to Whitmore criterion.

The length of a virtual column is computed as the average of L_1, L_2 and L_3, given in Fig. 8. Each of them is limited by AB line and clamped edges of gusset plate. Buckling coefficient of 0.65 may be assumed.

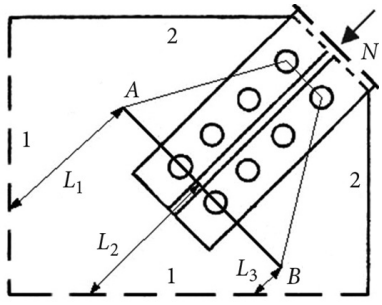

Fig. 8. Design of gusset plate in compression: 1 – clamped edge; 2 – free edge

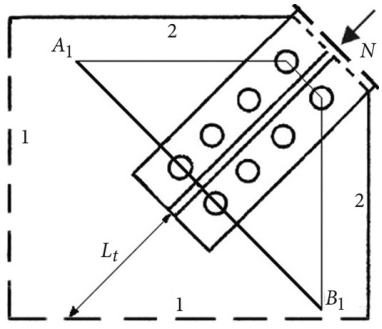

Fig. 9. Design of gusset plate in compression that yields prior to buckling: 1 – clamped edge; 2 – free edge

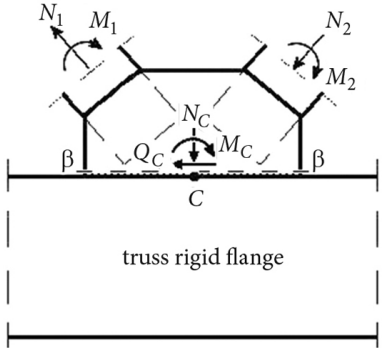

Fig. 10. Method of computation of stresses in gusset plate along β-β section

Simplified method of design of gusset plates under assumption that they buckle after yielding is also available (Yam, Cheng 1994). This method takes into account stress redistribution in gusset plate after its yielding but before buckling. It is shown in Fig. 9.

The angle of stress propagation is assumed here as 45° and A_1B_1 line coincides with last rivet/bolt row. Virtual column length may be taken as L_t (Fig. 9) or according to Thornton method. The approach shown in Fig. 9 may be applied under condition that elastic buckling strength is at least 50% higher than compressive strength computed according to Whitmore criterion that neglects buckling.

There are very few proposals of design of gusset plates under compression that go beyond column analogy (Sheng *et al.* 2002).

In general, the methods of gusset plate design consider single member connected to a gusset plate. Any interactions of adjacent members connected to the same gusset plate are reflected in a simplified manner. Moreover the methods are meant to assess the load carrying capacity of gusset plates instead if extreme stress level and stress distribution. Hence, they can hardly be applied to fatigue design.

2.2. Equivalent stress analysis

Classic method of assessment Huber-Mises (H-M) equivalent stress in gusset plate near its welded connection to truss flange requires computation of internal forces in bracing members. This may be easily accomplished based on analysis of beam-element FEM. The analysis results – internal forces N_1, M_1 and N_2, M_2 – are shown in Fig. 10. Shear forces in bracing members are usually very small and they are usually neglected. This does not affect further analysis.

Finding stresses along gusset plate to rigid flange connection (β-β section) requires computation of resultant normal force (N_C), resultant shear force (Q_C) and resultant bending moment (M_C), at the centre of gravity of butt welds – point "C" in Fig. 3.

The stress state at the β-β section is usually computed in the following way:

– normal stress:

$$\sigma_\beta = \frac{N_C}{A_\beta} + \frac{M_C}{J_\beta} y, \tag{4}$$

– shear stress:

$$\tau_\beta = \frac{Q_C}{A_\beta}, \tag{5}$$

– H-M equivalent stress:

$$\sigma_{equ.\beta} = \sqrt{\sigma_\beta^2 + 3\tau_\beta^2}, \tag{6}$$

where σ_β – normal stress at the β-β cross-section, MPa; τ_β – shear stress at the β-β cross-section, MPa; $\sigma_{equ\beta}$ – H-M equivalent stress at the β-β cross-section, MPa; A_β – cross-sectional area of the β-β cross-section, m^2;

J_β – moment of inertia of the β-β cross-section, m^4; y – distance between analysed fibre and centre of gravity of the β-β section, m.

3. Finite element analysis of gusset plates

FEM allows for accurate analysis of stress distribution in gusset plates. It makes it possible to respect actual dimensions of gusset plates and connected members as well as any details of bolting or welding.

There are various techniques of FEM analysis of stress distribution within gusset plates. They incorporate one-, two- or three-dimensional finite elements (Fig. 11), separately or combined. The techniques are:

– creating a brick-element model of a truss girder;
– creating a shell-element model of a truss girder;
– creating a hybrid model of a truss girder;
– applying multi-stage analysis.

Brick-element modelling of a truss girder. This is the most accurate technique. All steel sheets of structural members and all connection details (bolts and welds) are directly respected in such model. However, model preparation and result analysis are time consuming and require certain experience. This modelling technique is applied rather seldom.

Shell-element modelling of a truss girder. In this technique shell elements are applied to model steel sheets of truss girder members and gusset plates. Modelling of connectors (bolts and welds) is usually simplified or neglected. In spite of it this technique is able to pick main features of any stress distribution within gusset plates and thus it is applied pretty often (Crosti, Duthinh 2014; Kasano *et al.* 2012; Kumar *et al.* 2015; Lumpkin *et al.* 2012; Roeder *et al.* 2011).

Hybrid modelling of a truss girder. This technique is based on division of the analysed truss girder into regions of interest, i.e. joints, and "secondary" ones that need to be modelled to respect general structural behaviour. The former ones are modelled more accurately while the latter – in a simplified way (Li *et al.* 2009). For example: joints are modelled with shell elements and truss members – with beam elements. Compatibility of displacements must be ensured at the member cross-sections where different types of modelling meet each other.

Multi-stage analysis. This technique follows the idea of mixed modelling, however in a different way. It incorporates a simplified model of a truss girder and a more sophisticated model of the analysed joint. Firstly, the simplified model of a truss girder is analysed to find internal forces in members connected at the analysed joint. Secondly accurate model of the joint is created, for example with shell or brick elements, and its analysis is performed taking computed forces as boundary conditions. Such approach to joint analysis is rather tedious and nowadays less and less popular.

4. Lab testing of scaled bridge truss girder

Test of scaled bridge truss girder was carried out in the Institute of Civil Engineering of Poznań University of Technology. One of its aims was to assess stress distribution in gusset plate of rigid flange of bridge truss girder.

Test layout is shown in Fig. 12 and tested girder – in Fig. 13. The girder consists of hot rolled I-section members: HEA180 (top flange), HEA140 (bottom flange) and HEA100 (bracing members). The top flange is intended to behave as a rigid flange. Gusset plates are welded to flanges and bracing members are bolted to the plates with HSFG (high strength friction grip) bolts. At each joint, rigid flange is stiffened with three pairs of ribs. Figs 14 and 15 show the analysed joint.

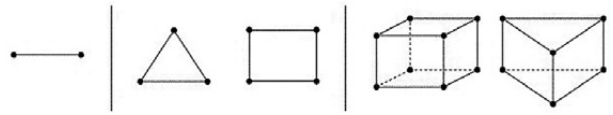

Fig. 11. Finite elements: beam (left), shell (middle), brick (right)

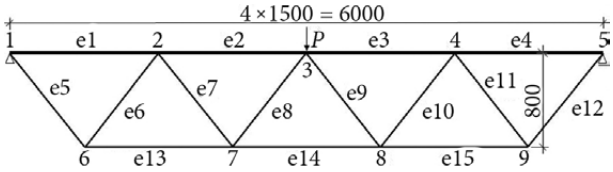

Fig. 12. General layout of test

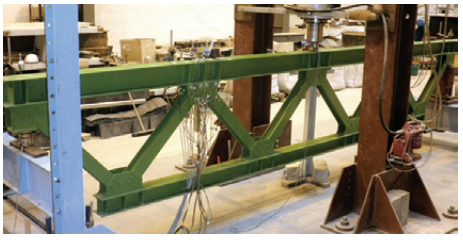

Fig. 13. Tested scaled model of truss girder

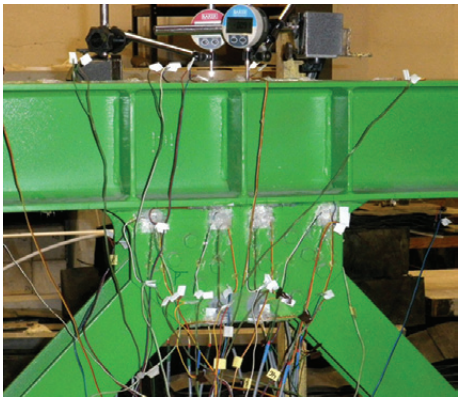

Fig. 14. Analysed joint – side view

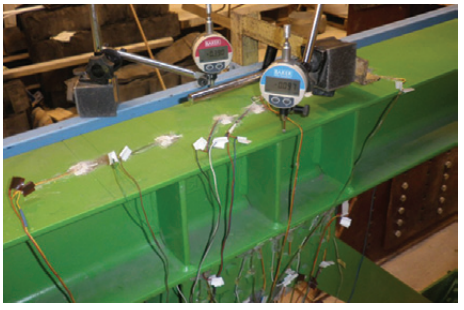

Fig. 15. Analysed joint – top view

Testing procedure consisted of several cycles $P = 0 \rightarrow 160 \rightarrow 0$ kN. Preliminary numerical analysis proved that under P = 160 kN loading the highest value of H-M equivalent stress in the girder stayed within elastic range.

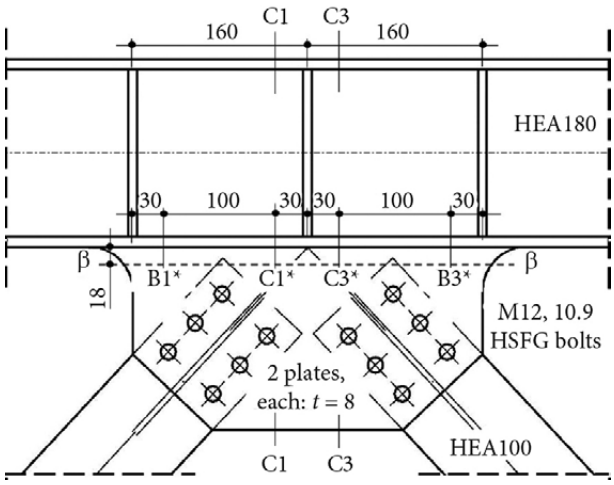

Fig. 16. Analysed cross-sections at node 2 (Fig. 12)

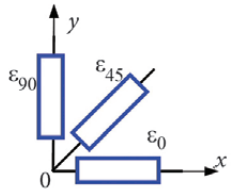

Fig. 17. Scheme of a rosette on twin gusset plates at B1*, C1*, C3*, B3*; ε_0, ε_{45}, ε_{90} denote measured strains

Table 1. Normal stress parallel to bracing members

Location	C1*	C3*
Normal stress, MPa	direction || to respective bracing	
	–35.6	26.5

Table 2. Normal stress values

Location	Normal stress	
	C1-C1	C3-C3
HEA180 top flange	–32.0	–31.6
HEA180 bottom flange	–10.6	–20.1
Gusset plate bottom edge	–5.0	15.8

Table 3. H-M equivalent stress values

Location (β-β)	B1*	C1*	C3*	B3*
Equivalent stress, MPa	18.7	54.4	59.1	39.3

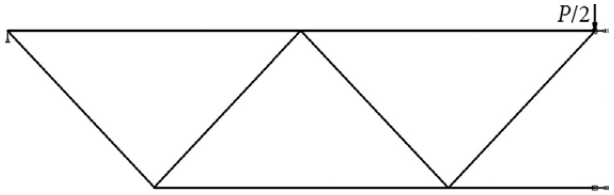

Fig. 18. Model B

Amongst other, the following were recorded:

– displacement of top flange nodes (marked 1–6 in Fig. 12),

– strains at C1-C1, C3-C3 and β-β cross-sections in the vicinity of the node 2 in Fig. 12 (the sections are shown in Fig. 16).

Displacements were recorded by means of Baker mechanical gauges of measurement resolution of 0.001 mm and strains – by means of HBM electrical gauges (unidirectional 1-LY-6/120 and 0°/45°/90° rosettes 1-RY11-6/120). Unidirectional gauges were located over top and bottom flanges of HEA180 and near bottom edge of gusset plate at sections C1-C1 and C3-C3.

Displacement and strain recordings proved elastic behaviour of the analysed girder.

On the basis of recorded strains the stresses were computed in following way:

– normal stresses:

$$\sigma_x = E\varepsilon_x, \tag{7}$$

– equivalent stresses σ_{red} (Fig. 17):

$$\sigma_{red} = \sqrt{\sigma_{11}^2 + \sigma_{22}^2 - \sigma_{11}\sigma_{22}}, \tag{8}$$

where the main stresses are:

$$\sigma_{11} = E\left(\frac{\varepsilon_0 + \varepsilon_{90}}{2} + \frac{\sqrt{2}}{2}\sqrt{\left(\varepsilon_0 - \varepsilon_{45}\right)^2 + \left(\varepsilon_{45} - \varepsilon_{90}\right)^2}\right), \tag{9}$$

$$\sigma_{22} = E\left(\frac{\varepsilon_0 + \varepsilon_{90}}{2} + -\frac{\sqrt{2}}{2}\sqrt{\left(\varepsilon_0 - \varepsilon_{45}\right)^2 + \left(\varepsilon_{45} - \varepsilon_{90}\right)^2}\right), \tag{10}$$

Table 1 gives normal stress in gusset plate, parallel to bracing members, at C1* and C3* locations, Table 2 gives normal stress in C1-C1 and C3-C3 cross sections and Table 3 gives H-M equivalent stress in the gusset plate, at B1*, C1*, C3* and B3* locations.

5. Numerical analysis

Two numerical models of the tested girder were created:

a) beam-element model, marked B (Fig. 18),

b) shell-element model, marked S (Fig. 19).

Model B was analysed in the Autodesk Robot environment while model S was analysed using Abaqus package, installed in Poznan Supercomputing and Networking Centre. For both models linearly-elastic material behaviour and small strain assumptions were made.

Model B (Fig. 18) was created with 2-node beam elements using linear interpolation. Half of the span of the analysed girder was considered. Truss members were assumed to have constant stiffness along their theoretical length, i.e. nodes were assumed to be dimensionless. Eccentricities of flange members location were respected.

Model S (Fig. 19) followed contemporary way of bridge truss girder modelling. It was created with 4-node

general-purpose shell elements with hourglass control. They were used to model truss member and gusset plates. The model S included half of the girder – whole span but up to longitudinal symmetry plane. Joint detail in this model is shown in Fig. 20.

2-node, linear interpolation beam elements were used to model bolts (Fig. 21):

– a group of elements in line, along shank axis (dashed line),

– a group of radial elements at the plane of contact between bolt head (nut) and outer steel plate surface (thick continuous line).

Contact was assumed over respective surfaces of bracing member walls and gusset plates bolted together as well as between end nodes of radial elements, modelling bolt head, and outermost steel plate surface. Friction coefficient was taken as $\mu = 0.45$.

Bolt pretension was modelled by means of Abaqus Pre-Tension Section command. In this way bolt pretension force was applied directly. Pretension force for M12 10.9 class bolts was assumed after Polish standard concerning steel bridges (*PN-82/S-10052, Bridges, Loads*), as 56.6 kN. According to *EN 1993-1-8:2006 Eurocode 3: Design of Steel Structures. Part 1-8: Design of Joints*, the pretension force for M12 10.9 class bolts is 59.0 kN.

For both analysed models appropriate kinematical constraints were applied at nodes located in symmetry planes. Since half of the girder was modelled, single concentrated load $P = 80$ kN was applied. In the case of model B the load was applied to the node in the centre of truss top flange. For model S the load was distributed over group of nodes in the vicinity of the node in the centre of truss top flange (piston cross-section dimensions were respected).

6. Computation of stresses

In the case of model S, normal and equivalent stress values were taken from output files directly.

For model B, stress values at the C1-C1 and C3-C3 cross-sections were computed as follows:

$$\sigma = \frac{N_B}{A_{joint}} + \frac{M_B + N_B e}{J_{joint}} z, \tag{11}$$

where N_B – axial force at the analysed cross-section, kN; M_B – bending moment at the analysed cross-section, kNm; A_{joint} – cross-sectional area of respective joint cross-section (Fig. 22), m^2; J_{joint} – moment of inertia of respective joint cross-section (Fig. 22), m^4; e – the distance between HEA180 and joint centres of gravity (in the analysed case it is 62 mm), m; z – the distance between centre of gravity of respective section and analysed fibre, m.

For model B, equivalent stresses at the β-β cross-section were computed according to the Eqs (7)–(9). Two different methods of shear stress computation were considered:

a) the simplified one (marked "model B") that assumed uniform distribution of shear stress:

$$\tau_\beta = \frac{Q_C}{A_\beta}, \tag{12}$$

b) the accurate one (marked "model B*") that respected non-uniform distribution of shear stress:

$$\tau_\beta = \frac{Q_C S_\beta}{J_\beta t}. \tag{13}$$

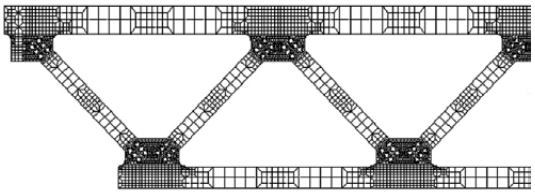

Fig. 19. Model S (up to symmetry plane)

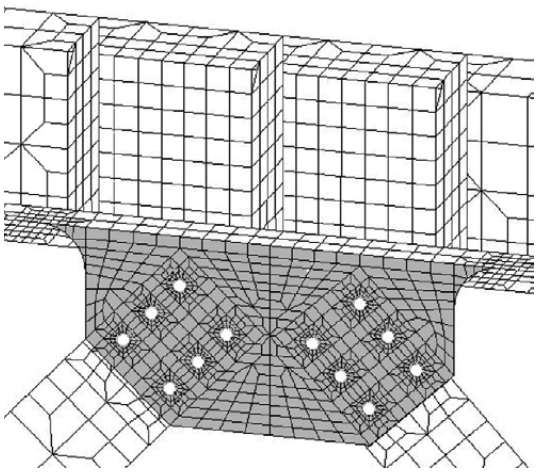

Fig. 20. Joint detail in the S model (gusset plate shaded, elements modelling bolts omitted)

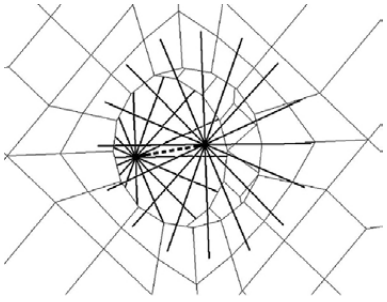

Fig. 21. Bolt model detail in shell-element model

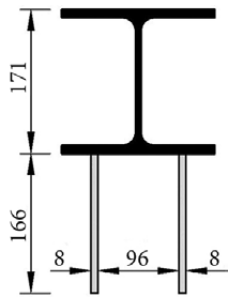

Fig. 22. Joint cross-sections: C1-C1 and C3-C3 (HEA180 and twin gusset plates)

The symbols in Eqs (15) and (16) are: Q_C – shear force at the β-β cross-section, A_β, J_β are cross-sectional area and second moment of area of the β-β cross-section, S_β – first moment of area of part of the β-β cross-section from its edge to the point where shear stress is computed, t – total thickness of twin gusset plates.

Table 4. Average stress estimation errors

Source	Average error δ_{ave} of estimation of			
	$\sigma_{\|\|}$	$\sigma_{C1\text{-}C1}$	$\sigma_{C3\text{-}C3}$	$\sigma_{equ\ \beta\text{-}\beta}$
Model B	25%	91%	28%	46%
Model B*				18%
Model S	14%	16%	8%	11%

Table 5. Normal stress parallel to bracing members

Source	$\sigma_{\|\| \text{ left}}$ (at C1*)	$\sigma_{\|\| \text{ right}}$ (at C3*)
Recorded	–35.6	26.5
Model B	–38.4	37.5
Model S	–37.4	28.3

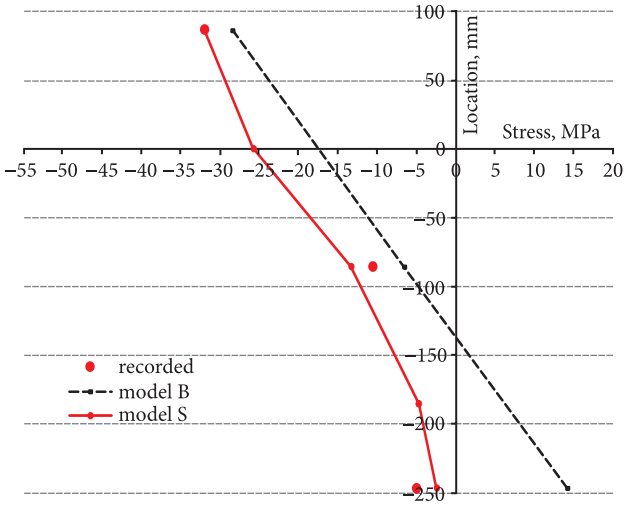

Fig. 23. Normal stress in C1-C1 cross-section

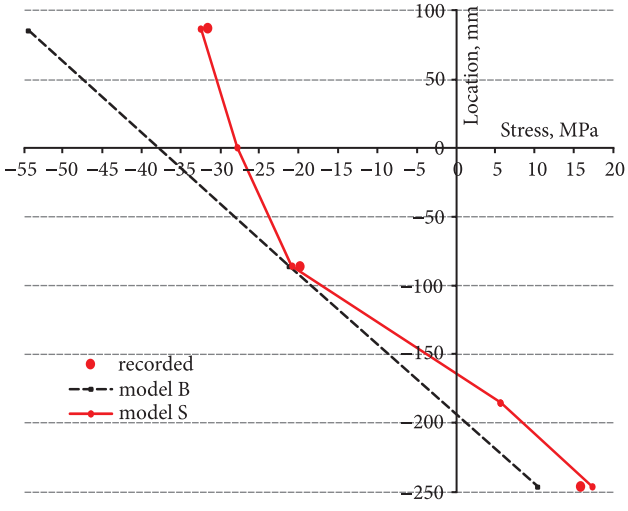

Fig. 24. Normal stress in C3-C3 cross-section

7. Computational results versus recorded data

To compare recorded and computed stress values an estimation error δ_k for the stress value at *k-th* location is introduced. It equals:

$$\delta_k = \left| \frac{\sigma_{comp(k)} - \sigma_{rec(k)}}{\sigma_{rec(k)}} \right|, \tag{14}$$

where $\sigma_{comp(k)}$, $\sigma_{rec(k)}$ – computed and recorded stress at *k-th* location at the cross-section in question, MPa.

Table 4 gives estimation error of stress assessment provided by models B and S. The meaning of the symbols: $\sigma_{||}$ – normal stress in gusset plate in the direction of respective bracing (left or right) near its tip, MPa; $\sigma_{C1\text{-}C1}$ – normal stress at the C1-C1 section, MPa; $\sigma_{C3\text{-}C3}$ – normal stress at the C3-C3 section, MPa; $\sigma_{equ\ \beta\text{-}\beta}$ – H-M equivalent stress at the β-β section, MPa.

The average estimation error δ_{ave} in analysed cross-sections is computed as:

$$\delta_{ave} = \sum_{k=1}^{n} \frac{\delta_k}{n}, \tag{15}$$

where n – amount of recorded strains in the cross-section in question; δ_k – estimation error of stress at *k-th* location in the cross-section in question.

Table 4 shows that Whitmore criterion gives satisfactory estimation of s|| stresses. Estimation errors for $\sigma_{C1\text{-}C1}$ stress and $\sigma_{C3\text{-}C3}$ stress in model B are significantly bigger than in model S. Estimation errors for $\sigma_{equ\ \beta\text{-}\beta}$ stresses show that non-uniform distribution of shear stress in given cross-section should be made while using output data form model B. The errors of $\sigma_{equ\ \beta\text{-}\beta}$ estimation in models B* and S are similar.

Table 5 gives recorded and computed normal stress values in gusset plate in the direction of respective bracing near truss theoretical node. In the case of model B the stress is computed on the basis of the Whitmore criterion. In the case of model S it is computed on the basis of stress field in elements modelling gusset plate.

Table 5 shows that model S gives the most accurate stress estimation. All models overestimate normal stress in gusset plate in the direction of respective bracing near its tip.

Figures 23 and 24 show normal stress distributions at the C1-C1 and C3-C3 cross-sections respectively. Estimations provided by models B and S are considered. The zero coordinate on vertical axis refers to neutral axis of HEA180 member. Coordinates +85.5 and –85.5 refer to the member top and bottom edge fibres of the flange members and –246.5 – to the bottom edge fibre of the gusset plate. Positive stress denotes tension.

Data given in Table 1 as well as in Figs 23 and 24 lead to the following remarks:

– normal stress distribution in the joint cross-sections, perpendicular to truss flange axis, is nonlinear;

– extreme normal stresses occur at cross-section edges;

– model B assessment of stress distribution is not accurate and may lead to under- or overestimation, especially near cross-section edges;

– model S, which incorporates simplified bolt modelling, gives very good assessment of stress distribution.

Fig. 25 shows distribution of equivalent stress in the β-β section. Estimations provided by models B, S and B* are considered. The zero ordinate on horizontal axis refers to location of truss theoretical node. Ordinates –150 and +150 refer to edge regions of gusset plate.

Data given in Table 4 and in Fig. 25 lead to the following observations:

– normal stress distribution in the section of gusset plate near its connection to truss rigid flange is nonlinear;

– extreme equivalent stress occurs near the centre of the β-β section;

– model B assessment of stress distribution estimates extreme stress values and their location with significant errors;

– model B* assessment is significantly better in comparison to model B in terms of location and value of extreme stress;

– model S gives good assessment of equivalent stress distribution;

– simplified bolt modelling applied in model S does not falsify the assessment of stress values in gusset plate.

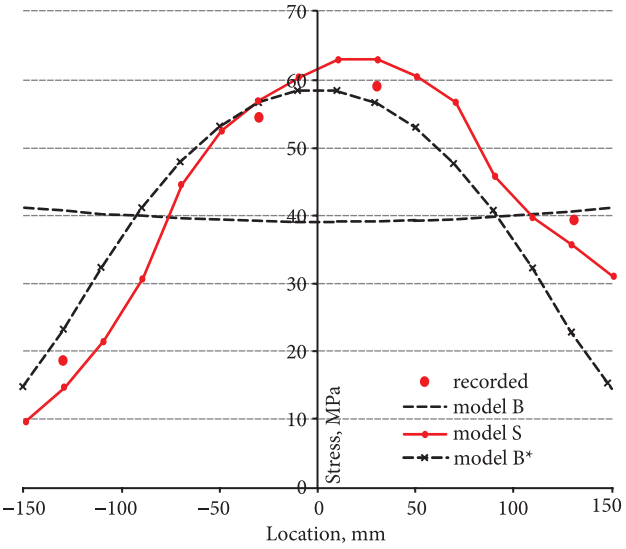

Fig. 25. H-M equivalent stress in β-β cross-section

8. Conclusions

1. Normal stress distribution in gusseted joint cross-section, perpendicular to truss flange axis, is nonlinear. Extreme stresses occur near cross-section edges.

2. Huber-Mises equivalent stress distribution at the cross-section of a gusset plate near its connection to truss flange is nonlinear. Extreme stresses occur near centre of the cross-section.

3. Assessment of normal stresses in gusseted joints should not be carried out with an aid of beam-element modelling.

4. It is possible to assess Huber-Mises equivalent stresses in gusset plate near its welded connection to rigid flange with an aid of beam-element modelling. To do so non-uniform distribution of shear stress must be taken into account.

5. Shell-element modelling of gusseted joint provides satisfactory accuracy of normal and equivalent stress assessment.

6. Beam-element modelling of friction grip bolts is sufficiently accurate for shell-element models of steel joints analysed within elastic range of behaviour.

References

Ahlgrimm, J.; Lohrer, I. 2005. Erneuerung der Eisenbahnüberführung in Fulda-Horas über die Fulda [A New Rail Bridge Crosses the River Fulda in Fulda-Horas], *Stahlbau* 74(2): 114–120. http://dx.doi.org/10.1002/stab.200590002

Kumar, A.; Mannan, A.; Anand, A.; Sahoo, D. R. 2015. Study on the in-Elastic Performance of Mid-Span Gusset Plate Used in Concentrically Braced Frames, in *Proc. of the 10th Pacific Conference on Earthquake Engineering Building an Earthquake-Resilient Pacific*, 6–8 November 2015, Sydney, Australia.

Berman, J.; Wang, B.; Roeder, C.; Olson, A.; Lehman, D. 2010. *Triage Evaluation of Gusset Plates in Steel Truss Bridges*. Research Project T4118, Washington State Transportation Center. 81 p.

Chou, C.; Chen, P. 2009. Compressive Behavior of Central Gusset Plate Connections for a Buckling-Restrained Braced Frame, *Journal of Constructional Steel Research* 65(5): 1138–1148. http://dx.doi.org/10.1016/j.jcsr.2008.11.004

Crosti, C.; Duthinh, D. 2014. A Nonlinear Model for Gusset Plate Connections, *Engineering Structures* 62–63: 135–147. http://dx.doi.org/10.1016/j.engstruct.2014.01.026

Crosti, C.; Duthinh, D. 2012. Simplified Gusset Plate Model for Failure Prediction of Truss Bridges, in *Bridge Maintenance, Safety, Management, Resilience and Sustainability*. Ed by Biondini, F; Frangopol, D. M., 1415–1419, Taylor & Francis Group, London. 4057 p. http://dx.doi.org/10.1201/b12352-202

Hardash, S. G.; Bjorhovde, R. 1985. New Design Criteria for Gusset Plates in Tension, *AISC Engineering Journal* 22(2): 77–94.

Kaneko, K.; Kasai, K.; Motoyui, S.; Sueoka, T.; Azuma, Y.; Ooki, Y. 2008. Analysis of Beam-Column-Gusset Component in 5-Storey Value-Added Frame, in *The 14th World Conference on Earthquake Engineering*, 12–17 October 2008, Beijing, China.

Kasano, H.; Yoda, T.; Nogami, K.; Murakoshi, J.; Toyama, N.; Sawada, M.; Arimura, K.; Guo, L. 2012. Study on Failure Modes of Steel Truss Bridge Gusset Plates Related to Tension and Shear Block Failure, *International Journal of Steel Structures* 12(3): 381–389. http://dx.doi.org/10.1007/s13296-012-3007-5

Li, Z. X.; Chan, T. H. T.; Yu, Y.; Sun, Z.H. 2009. Concurrent Multi-Scale Modelling of Civil Infrastructures for Analyses on Structural Deterioration – Part I: Modelling Methodology and Strategy, *Finite Elements in Analysis and Design* 45(11): 782–94. http://dx.doi.org/10.1016/j.finel.2009.06.013

Lumpkin, E.; Hsiao, P.; Roeder, C.; Lehman, D.; Tsai, C.; Wu, A.; Wei, C.; Tsai, K. 2012. Investigation of the Seismic Response of Three-Story Special Concentrically Braced Frames, *Journal of Constructional Steel Research* 77: 131–144. http://dx.doi.org/10.1016/j.jcsr.2012.04.003

Najjar, W.; DeOrtentiis, F. 2010. Gusset Plates in Railroad Truss Bridges – Finite Element Analysis and Comparison with

Whitmore Testing, *Annual Conference of American Railway Engineering and Maintenance-of-Way Association (AREMA)*, 29 August – 1 September 2011, Orlando, USA.

Reintjes, K.; Gebert, G. 2006. Das Zügelgurt-Fachwerk der Muldebrücke Wurzen [The Truss–Stayed Structure of the Mulde Bridge Wurzen], *Stahlbau* 75(8): 613–623. http://dx.doi.org/10.1002/ stab.200610063

Roeder, C.; Lumpkin, E.; Lehman, D. 2011. A Balanced Design Procedure for Special Concentrically Braced Frame Connections, *Journal of Constructional Steel Research* 67(11): 1760–1772. http://dx.doi.org/10.1016/j.jcsr.2011.04.016

Rosenstrauch, P. L.; Sanayei, M.; Brenner, B. R. 2013. Capacity Analysis of Gusset Plate Connections Using the Whitmore, Block Shear, Global Section Shear, and Finite Element Methods, *Engineering Structures* 48: 543–557. http://dx.doi.org/10.1016/j.engstruct.2012.08.032

Sheng, N.; Yam, C. H.; Iu, V. P. 2002. Analytical Investigation and the Design of the Compressive Strength of Steel Gusset Plate Connections, *Journal of Constructional Steel Research* 58(11): 1473–1493. http://dx.doi.org/10.1016/S0143-974X(01)00076-1

Szelągowski, F. 1966. Mosty metalowe, część I [Metal Bridges. Part I], WKŁ, Warszawa. 573 p.

Thornton, W. A. 1984. Bracing Connections for Heavy Constructions, *Engineering Journal* 3: 139–148.

Whitmore, R. E. 1952. Experimental Investigation of Stresses in Gusset Plates, *Engineering Experiment Station Bulletin* 16, University of Tennessee.

Yam, M. C. H.; Cheng, J. J. R. 1994. Analytical Investigation of the Compressive Behaviour and Strength of Steel Gusset Plate Connections, *Structural Engineering Report* 207, University of Alberta.

Yoo, J.; Lehman, D.; Roeder, C. 2008. Influence of Connection Design Parameters on the Seismic Performance of Braced Frames, *Journal of Constructional Steel Research* 64: 607–623. http://dx.doi.org/10.1016/j.jcsr.2007.11.005

Zhang, W.; Huang, M.; Zhang, Y.; Sun, Y. 2011. Cyclic Behaviour Studies on I-Section Inverted V-Braces and Their Gusset Plate Connections, *Journal of Constructional Steel Research* 67(3): 407–420. http://dx.doi.org/10.1016/j.jcsr.2010.09.012

Zongyu, G. 2012. Zhengzhou Yellow River Road-Cum-Railway Bridge, China, *Stahlbau* 81(2): 151–155. http://dx.doi.org/10.1002/stab.201201522

Received 15 May 2013; accepted 9 January 2014